Improving Contrast and Detectability: Imaging with [^{55}Co]Co-DOTATATE in Comparison with [^{64}Cu]Cu-DOTATATE and [^{68}Ga]Ga-DOTATATE

Thomas L. Andersen[1,2], Christina Baun[1], Birgitte B. Olsen[1,2], Johan H. Dam[1,2], and Helge Thisgaard[1,2]

[1]*PET Unit, Department of Nuclear Medicine, Odense University Hospital, Odense, Denmark; and* [2]*Department of Clinical Research, University of Southern Denmark, Odense, Denmark*

PET imaging at late time points after injection may allow tracer clearance from normal tissue and hence improve image contrast and detectability. ^{55}Co is a promising isotope with high positron yield and a long half-life suitable for imaging at delayed time points. Here, we compared the 3 radioconjugates [^{68}Ga]Ga-DOTATATE, [^{64}Cu]Cu-DOTATATE, and [^{55}Co]Co-DOTATATE by PET/CT imaging in NOD-SCID mice bearing subcutaneous somatostatin receptor–expressing AR42J tumors. **Methods:** ^{55}Co and ^{64}Cu were produced by the ^{54}Fe(d,n)^{55}Co and ^{64}Ni(p,n)^{64}Cu nuclear reactions, whereas ^{68}Ga was obtained from a ^{68}Ge/^{68}Ga generator. ^{55}Co and ^{64}Cu were labeled with DOTATATE by heating in a sodium acetate buffer and 4-(2-hydroxyethyl)-1-piperazineethanesulfonic acid buffer, respectively. AR42J tumor–bearing mice were dynamically scanned 0–1 h after injection. For ^{64}Cu and ^{55}Co, additional imaging was also performed at late time points after 4 and 24 h. Dose calculations were based on a known biodistribution. The cumulated disintegrations in each organ were calculated by integration of a fitted exponential function to the biodistribution of each respective organ. Equivalent doses were calculated by OLINDA/EXM using the MIRD formalism. **Results:** Tumor uptake was rapid from 0 to 1 h after injection for all 3 radioconjugates. Normal-tissue ratios as represented by tumor-to-liver, tumor-to-kidney, and tumor-to-muscle ratios increased significantly over time, with [^{55}Co]Co-DOTATATE reaching the highest ratio of all radioconjugates. For [^{55}Co]Co-DOTATATE, the tumor-to-liver ratio increased to 65 ± 16 at 4 h and 50 ± 6 at 24 h, which were 15 ($P < 0.001$) and 30 ($P < 0.001$) times higher, respectively, than the corresponding ratios for [^{64}Cu]Cu-DOTATATE and 5 ($P < 0.001$) times higher than that of [^{68}Ga]Ga-DOTATATE at 1 h. Correspondingly, tumor-to-kidney and tumor-to-muscle ratios for [^{55}Co]Co-DOTATATE were 4 ($P < 0.001$) and 11 ($P < 0.001$) times higher than that of [^{64}Cu]Cu-DOTATATE at 24 h. An equivalent dose was calculated as 9.6E−02 mSv/MBq for [^{55}Co]Co-DOTATATE. **Conclusion:** [^{55}Co]Co-DOTATATE demonstrated superior image contrast compared with [^{64}Cu]Cu-DOTATATE and [^{68}Ga]Ga-DOTATATE for PET imaging of somatostatin receptor–expressing tumors, warranting translation into clinical trials. Dosimetry calculations found that effective doses for [^{55}Co]Co-DOTATATE were comparable to those for both [^{64}Cu]Cu-DOTATATE and [^{68}Ga]Ga-DOTATATE.

Key Words: DOTATATE; neuroendocrine tumor; ^{64}Cu; ^{55}Co; ^{68}Ga

J Nucl Med 2020; 61:228–233
DOI: 10.2967/jnumed.119.233015

Neuroendocrine tumors represent a broad heterogeneous group of malignancies. For diagnostic workup and treatment response monitoring, imaging by both functional and anatomic modalities has played a vital role. For functional molecular imaging, the somatostatin receptor (SSTR) has been found to be overexpressed in most neuroendocrine tumors (NETs) (*1*), paving the way for functional imaging by targeting SSTR. Historically, functional molecular imaging of SSTRs has been performed with SPECT, using somatostatin analogs labeled first with ^{123}I (*2*) and subsequently with ^{111}In (*2,3*) and ^{99m}Tc (*4*). With the advent of clinical PET scanners offering higher sensitivities and higher spatial resolution, peptides labeled with positron emitters such as ^{68}Ga, ^{18}F, ^{86}Y, and ^{64}Cu have been investigated (*5–9*). Currently, ^{68}Ga has attracted most of the attention because of its positron yield of 89% and half-life of 68 min, which match the pharmacokinetics of many peptides. ^{68}Ga is also readily available from the ^{68}Ge/^{68}Ga generator, with the parent isotope, ^{68}Ge, having a half-life of 270.8 d, which reduces the generator exchange to 1–2 times per year. Moreover, the relatively simple labeling procedure has further pushed the use of [^{68}Ga]Ga-DOTATOC, [^{68}Ga]Ga-DOTATATE, and [^{68}Ga]Ga-DOTANOC to become the standard for functional molecular imaging in NETs. Although SSTR is the general targeted receptor, the 3 somatostatin analogs have distinct affinity profiles for SSTR subtypes. Of these analogs, [^{68}Ga]Ga-DOTATATE exhibits the highest affinity toward SSTR subtype 2 (SSTR2) (*10*), which is the predominant subtype in NETs.

Besides development of new targeting molecules and analogs, large affinity differences have been observed in SSTR tracers that are identical but labeled with different isotopes (*11*). This has given rise to an increasing interest in radiotracer labeling with radiometals other than ^{68}Ga. In this respect, Reubi et al. (*12*) found a half-maximal inhibitory concentration of 11.7 ± 1.7 nM and 2.5 ± 0.5 nM for Y-DOTATOC and Ga-DOTATOC, respectively, for SSTR2, whereas respective values of 1.6 ± 0.4 nM and 0.2 ± 0.04 nM were reported for Y-DOTATATE and Ga-DOTATATE, demonstrating large affinity differences for identical vectors but different isotopes in cell lines transfected with SSTR subtypes. These results were extended by Heppeler et al. (*13*), who synthesized and

Received Jun. 27, 2019; revision accepted Aug. 15, 2019.
For correspondence or reprints contact: Helge Thisgaard, Department of Nuclear Medicine, Odense University Hospital, Kløvervænget 47, indg. 44-46, DK-5000 Odense C, Denmark.
E-mail: helge.thisgaard@rsyd.dk
Published online Sep. 13, 2019.

tested [^{57}Co]Co-DOTATOC as a surrogate for the positron-emitting radioconjugate [^{55}Co]Co-DOTATOC and found a half-maximal inhibitory concentration of 0.44 ± 0.11 nM, demonstrating, to our knowledge, the highest affinity seen toward SSTR2 in an AR42J tumor cell line. Further, DOTATOC, DOTANOC, and DOTATATE have been labeled with different cobalt isotopes (^{55}Co/^{57}Co or ^{58m}Co) for theranostic applications (*14*), where the cobalt-labeled DOTATATE showed the highest translocation to the cell nucleus (*15*). Compared with [^{177}Lu]Lu-DOTATATE, [^{58m}Co]Co-DOTATATE was significantly more efficient in cell killing per cumulated decay, showing promise for a future theranostic pair using ^{55}Co/^{58m}Co.

Clinically, [^{64}Cu]Cu-DOTATATE has been introduced to overcome some of the shortcomings of [^{68}Ga]Ga-DOTA-X (*16*), such as the short half-life lowering the specific activity with time and the high β^+ energy resulting in low-resolution images. In this respect, [^{55}Co]Co-DOTATATE represents a promising candidate for NET imaging because of its physical half-life, allowing late-time-point imaging, and because of the high affinity for SSTR shown for Co-DOTATOC.

The purpose of this study was to perform a head-to-head comparison of [^{55}Co]Co-DOTATATE, [^{64}Cu]Cu-DOTATATE, and [^{68}Ga]Ga-DOTATATE and to characterize the in vivo imaging characteristics in a SSTR-positive xenografted mouse model.

MATERIALS AND METHODS

Isotope Production

^{68}Ga was obtained from a ^{68}Ge/^{68}Ga generator (Eckert and Ziegler), whereas ^{55}Co and ^{64}Cu were produced in-house using a PETtrace cyclotron. The production method for ^{55}Co has been described previously (*14,17*). Briefly, highly enriched ^{54}Fe was irradiated with 18 μA of 8.4-MeV deuterons for 6 h the day before labeling, followed by radiochemical separation using anion-exchange resin (Dowex 1·8; DuPont) and 4 M HCl as eluent, with further purification using a Chromafix 30-PS-HCO3 cartridge. ^{64}Cu was produced by proton bombardment of highly enriched ^{64}Ni using a fully automated solid-target irradiation system (QIS; ARTMS). The irradiation was performed with 60 μA of 13-MeV protons for 4 h. After the irradiation, the target capsule was pneumatically transferred to a hot cell and mounted in a dissolution cell for dissolving the ^{64}Cu/^{64}Ni using 6 M HCl. After the dissolution process, the resulting solution was transferred to a GE Healthcare FastLab 2 Developer programmed to automatically separate the ^{64}Cu from the ^{64}Ni target material using anion-exchange resin (AG 1-X8; Bio-Rad) and HCl as eluent (6.5, 4, and 0.01 M HCl).

Radiolabeling of DOTATATE

DOTATATE was purchased in good-manufacturing-practice grade from ABX GmBH. Radiolabeling with ^{68}Ga was performed by the standard Eckert-Ziegler cassette synthesis on the Modular Lab Pharm Tracer synthesis unit in connection with the sterile GalliPharm ^{68}Ge/^{68}Ga generator. Briefly, in-house–prepared kits of DOTATATE (28 nmol; ABX) in 4-(2-hydroxyethyl)-1-piperazineethanesulfonic acid buffer (0.75 M, pH 4.0–4.1, 2 mL) were radiolabeled with ^{68}Ga at 95°C for 400 s and then purified by standard C18 solid-phase extraction.

Radiolabeling with ^{55}Co was performed using 4.9 nmol of DOTATATE (1 μg/μL) buffered in 50 μL of sodium acetate (pH 4.6; Sigma-Aldrich). This precursor solution was mixed with the [^{55}Co]$CoCl_2$ (86 MBq in 50 μL of 0.04 M HCl) and heated to 90°C using dynamic PETwave microwave irradiation for 2 min.

Radiolabeling with ^{64}Cu was performed using 2.8 nmol of DOTATATE (1 μg/μL) buffered in 30 μL of sodium acetate (pH 4.6). This precursor solution was mixed with the [^{64}Cu]$CuCl_2$ (40 MBq in 20 μL of 0.01 M HCl) and left at room temperature for 10 min, after which the solution was loaded onto an Empore cartridge (4315SD), washed with 2 mL of water for injection, and eluted dropwise with aqueous ethanol (70%).

All radioconjugates were finally diluted with phosphate-buffered saline containing 0.1% bovine serum albumin. After dilution, a concentration of 9 vol% ethanol remained in [^{64}Cu]Cu-DOTATATE whereas below 2 vol% remained in [^{68}Ga]Ga-DOTATATE. No ethanol was used in the formulation of [^{55}Co]Co-DOTATATE.

Radiochemical purities were assessed using analytic reverse-phase high-performance liquid chromatography (Hitachi LaChrom Elite system and Phenomenex Jupiter C18 300A column, 150 × 4.60 mm; 5 μm) as previously described (*14*). [^{68}Ga]Ga- and [^{64}Cu]Cu-DOTATATE were further analyzed by instant thin-layer chromatography (Biodex 150-771) and eluted in 0.1 M citric acid on which radiometals elute with the solvent front.

In Vivo Animal Studies

Male NOD-SCID mice (n = 10) 7–9 wk old were used from an in-house breeding program. The mice were inoculated subcutaneously with 10^6 AR42J cells in a Matrigel-to-medium (Matrigel; Corning) ratio of 1:1 in the upper left flank. PET/CT scans were performed after confirmation that an approximately 5-mm tumor had developed as measured by an external caliper. Before scanning, the mice were anesthetized by 1.5%–2% isoflurane in 100% oxygen and placed prone on the scanner bed. All animal experiments were approved by the Animal Experiments Inspectorate in Denmark.

PET/CT scans were performed on a preclinical Inveon PET/CT scanner (Siemens Preclinical Solutions) in docked mode. Before the PET data acquisition, a CT scan was acquired with a full 360° rotation using 270 projections acquired with 80 kV and 500 μA exposures for subsequent attenuation and scatter correction use. List-mode data were reconstructed after scanning using a maximum a posteriori algorithm in conjunction with a 3-dimensional ordered-subset expectation maximum algorithm, giving a central resolution of approximately 1.5 × 1.5 × 1.5 mm.

The injected activity was varied in the mice to match peptide amounts across all groups. Accordingly, the mice were injected intravenously with activities between 1.7 MBq and 4.6 MBq, corresponding to 0.12 ± 0.02 nmol per animal. Four mice were scanned with [^{68}Ga]Ga-DOTATATE, 3 with [^{64}Cu]Cu-DOTATATE, and 3 with [^{55}Co]Co-DOTATATE.

All mice were scanned at 3 selected time points after injection, namely a dynamic scan at 0–1 h, a static scan at 4 h, and a static scan at 24 h. For [^{68}Ga]Ga-DOTATATE, the scans at 4 and 24 h were omitted because of the short physical half-life of ^{68}Ga.

All mice were awakened from anesthesia between longitudinal scans and allowed to roam freely in cages with unrestricted access to food and water.

Data Analysis

All PET/CT scans were analyzed using Inveon Research Workplace software (Siemens Preclinical Solutions). Tumors were segmented by applying a fixed 40% threshold of the maximum uptake. Muscle uptake volumes of interest were drawn freehand in the right anterior lower gastrocnemius muscle or alternatively in the upper left extensors in cases of high bladder uptake. Such high uptake in the bladder has a tendency to spill into the gastrocnemius muscle, making it poorly suited for a representative measure of background uptake. Additionally, both kidneys were segmented with a procedure akin to the tumor segmentation, whereas the liver was segmented as a freehand ellipsoidal volume of interest below the lungs (according to an anatomic atlas) because of the poor soft-tissue contrast on CT.

After segmentation, volume-of-interest means, SDs, and maximums were calculated. Furthermore, all data were decay-corrected between

longitudinal scans to facilitate direct comparison between different isotopes using half-lives of 12.7 h and 17.5 h for ^{64}Cu and ^{55}Co, respectively.

Dosimetry

Because of animal ethics, dosimetry calculations for [^{55}Co]Co-DOTATATE were based on a known biodistribution (*15*) published previously by our group for [^{57}Co]Co-DOTATATE. No kinetic distribution differences are expected between isotopes of the same element. The biodistribution for [^{57}Co]Co-DOTATATE is hence equal to that for [^{55}Co]Co-DOTATATE. The accumulated activity in the source organs, $\tilde{A}_h$, was calculated from the integration of activity in the source organs with time, $A_h(t)$

$$\tilde{A}_h = \int_0^\infty A_h(t)dt.$$

Source organ data were fitted by an exponential of the following form:

$$A_h(t) = \frac{A}{k_a - k_b} \times \left(e^{-k_b \cdot t} - e^{-k_a \cdot t}\right),$$

where k_b and k_a are uptake and elimination rates, respectively. Mice organ activity data were organ-to-mass scaled to human equivalents akin to a previous approach (*18*):

$$\tilde{A}_{h,o} = \tilde{A}_{a,o} \times \frac{O_{m,h}/m_h}{O_{m,a}/m_a},$$

where $\tilde{A}_{a,o}$ is the cumulated activity in the animal, $O_{m,(h,a)}$ is the organ mass in a normal human (*19*) and mouse, respectively, and $m_{(h,a)}$ is the total mass of a normal human and animal (25 g). Absorbed doses were calculated by the MIRD formalism (*20*) using *S* factors in the adult model as implemented in OLINDA/EXM 1.1 (*21*).

Statistical Analysis

Statistical analysis was performed in Prism, version 6 (GraphPad Software), using 2-way ANOVA and follow-up tests with either the Tukey or the Holm–Šídák approach to correct for multiple comparisons.

RESULTS

[^{68}Ga]Ga-DOTATATE was obtained in a yield of 841 ± 159 MBq (n = 6) and a radiochemical purity of 97.8% ± 0.3% at the end of synthesis. [^{64}Cu]Cu-DOTATATE was obtained in a radiochemical and radionuclidic purity above 99% (n = 1) at the end of synthesis. [^{55}Co]Co-DOTATATE was obtained in 99.5% yield and a radiochemical purity above 99.5% (n = 1) at the end of synthesis. The apparent molar activities at the end of synthesis were approximately 18, 16, and 41 MBq/nmol for [^{55}Co]Co-DOTATATE, [^{64}Cu]Cu-DOTATATE, and [^{68}Ga]Ga-DOTATATE, respectively. Quantitative imaging by PET/CT showed a rapid increase in tumor uptake from 0 to 60 min for all radioconjugates, reaching a maximum at 1–4 h after injection. The comparison of absolute uptake concentrations normalized to injected activity at 1, 4, and 24 h are shown in Figure 1A. Absolute uptake did not significantly differ between radioconjugates at equivalent time points, although a generally lower uptake was found for [^{68}Ga]Ga-DOTATATE. Late-time-point imaging as made possible by the longer half-life of both ^{55}Co and ^{64}Cu than of ^{68}Ga resulted in a higher tumor-to-kidney ratio as illustrated by Figure 1C.

Compared with 1 h after injection, the liver concentration was reduced by a factor of 9 at 24 h for [^{55}Co]Co-DOTATATE. Oppositely, the liver concentration for [^{64}Cu]Cu-DOTATATE increased slightly, but nonsignificantly, from 1 h to 24 h after injection, resulting in a generally lower tumor-to-liver ratio (Fig. 1B). For [^{55}Co]Co-DOTATATE, the tumor-to-liver ratio increased to 65 ± 16 at 4 h and 50 ± 6 at 24 h, which were 15 ($P < 0.0001$) and 29 ($P < 0.0001$) times higher, respectively, than the corresponding ratios for [^{64}Cu]Cu-DOTATATE and 5 ($P < 0.0001$) times higher than that for [^{68}Ga]Ga-DOTATATE at 1 h. Furthermore, the tumor-to-kidney ratio at 24 h for [^{55}Co]Co-DOTATATE was 4 ($P < 0.0001$) times higher than that for [^{64}Cu]Cu-DOTATATE and 8 ($P < 0.0001$) times higher than that for [^{68}Ga]Ga-DOTATATE at 1 h. Similarly, as a surrogate for background uptake, the tumor-to-muscle ratio at 24 h for [^{55}Co]Co-DOTATATE was 11 ($P < 0.0001$) times higher than that for [^{64}Cu]-DOTATATE and 8 ($P < 0.0001$) times higher than that for [^{68}Ga]Ga-DOTATATE at 1 h.

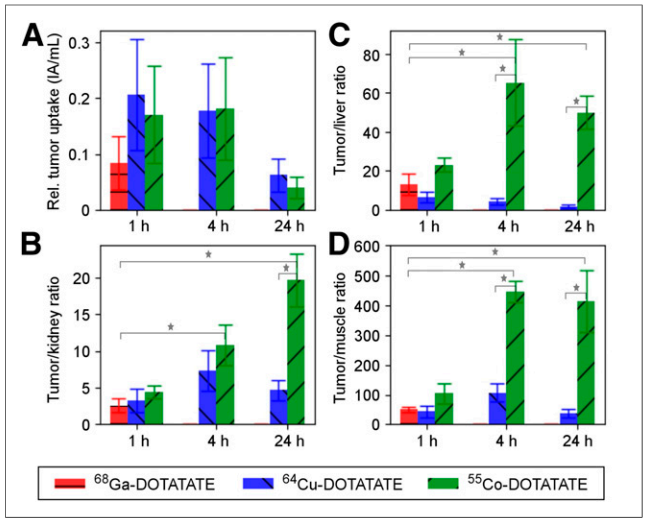

FIGURE 1. Tumor uptake and ratios to liver, kidneys, and muscle with SD error bars. Statistical significance ($P < 0.001$) is indicated by stars. No significant difference in tumor uptake was observed, whereas statistically significant differences were found among the 3 radioconjugates in all tumor–to–normal-tissue ratios. [^{55}Co]Co-DOTATATE showed the highest ratio in liver, kidneys, and muscle and showed highest tumor-to-liver and tumor-to-muscle ratio at 4 h after injection (Supplemental Table 1; supplemental materials are available at http://jnm.snmjournals.org).

Dosimetry calculations based on [^{57}Co]Co-DOTATATE as a surrogate for [^{55}Co]Co-DOTATATE are shown in Table 1.

From the organ source data, the effective dose equivalent was calculated to be 9.6E−02 mSv/MBq, with the highest individual doses being in the lungs, stomach, and kidneys, at 6.5E−02, 2.1E−02, and 7.2E−04 mSv/MBq, respectively (Table 1).

DISCUSSION

Improvement in image contrast and hence detectability of malignancies from PET imaging depends not only on finding new targeting mechanisms with new tracers but also on the imaging properties of the radionuclide. The development of new tracers by combining existing targeting mechanisms, such as SSTR analogs, but with isotopes with other radiophysical properties, can have a significant impact on diagnostic performance (*22,23*). In this respect, ^{55}Co is a promising isotope because of its high positron yield of 75.9% (*24*), compared with only 17.6% for ^{64}Cu (*25*), its suitable half-life of 17.53 h, and the demonstrated superior affinity for SSTR2 when bound to DOTATOC (*13*), which is the predominant overexpressed subtype in NETs. Further, combining ^{55}Co with the

TABLE 1
[^{55}Co]Co-DOTATATE Dosimetry Results Scaled to Adult Human from Co-DOTATATE Biodistribution

Organ	$\tilde{A}_{h,o}$ (h)	Effective dose (mSv/MBq)
Adrenals	0.002	3.2E−04
Kidneys	0.12	7.2E−04
Small intestine	0.13	2.8E−04
Liver	0.013	1.2E−03
Lungs	1.77	6.5E−02
Spleen	0.006	2.0E−04
Pancreas	0.03	6.5E−04
Stomach	0.24	2.1E−02
Effective dose		9.6E−02

therapeutic isotope ^{58m}Co, which is a known Auger electron emitter (*17*), a promising theranostic pair becomes apparent. Drawbacks of ^{55}Co are the high-energy γ-lines of 931.3 keV (75%), 1,316 keV (7.1%), and 1,408.4 keV (16.9%). These prompt γ-lines do not, however, influence image quality significantly on newer-generation PET scanners with modern reconstructions or time-of-flight capability (*26*), and ^{55}Co is therefore a viable option for routine clinical imaging with proper radiation protection.

Dosimetric calculations of [^{55}Co]Co-DOTATATE yielded an effective dose equivalent of 9.6E−02 mSv/MBq. For comparison, an effective dose of 3.2E−02 mSv/MBq has been reported for [^{64}Cu]Cu-DOTATATE on the basis of biodistributions in humans (*16*). Similarly, an effective dose of 2.1E−02 mSv/MBq has been reported for [^{68}Ga]Ga-DOTATATE (*27*). The effective dose for [^{55}Co]Co-DOTATATE is hence higher per injected activity than is the effective dose of [^{64}Cu]Cu-DOTATATE or [^{68}Ga]Ga-DOTATATE. However, the low positron yield of ^{64}Cu of only 17.6% requires higher amounts of administered activities to obtain diagnostic-quality images. Consequently, in the study by Pfeifer et al. (*16*), a mean injected activity of 207 MBq was used. To obtain the same equivalent number of annihilation events in identical scanners, the positron fraction must be normalized between ^{64}Cu and ^{55}Co. The ratio between positron yields from ^{64}Cu and ^{55}Co is 4.2 (0.76/0.18 = 4.2), suggesting that the injected activity of [^{55}Co]Co-DOTATATE should be a factor of 4.2 lower than that of [^{64}Cu]Cu-DOTATATE. Scaling the mean injected activity of [^{64}Cu]Cu-DOTATATE by 4.2 results in a projected injected activity of 49 MBq of [^{55}Co]Co-DOTATATE. An injected activity of 49 MBq corresponds to an effective total dose of 4.7 mSv, compared with a dose commitment of 6.5 mSv of [^{64}Cu]Cu-DOTATATE from an injected dose of 207 MBq. [^{55}Co]Co-DOTATATE dosimetry is hence comparable to [^{64}Cu]Cu-DOTATATE dosimetry from a patient-dosimetry point of view. [^{68}Ga]Ga-DOTATATE does indeed lower the effective dose if also adjusted for positron yield, but because of the relatively higher tissue uptake, [^{68}Ga]Ga-DOTATATE suffers from low contrast, and because of the short physical half-life, [^{68}Ga]Ga-DOTATATE does not allow for late-time-point imaging.

Another dosimetry aspect of ^{55}Co is the decay to ^{55}Fe, which is also unstable and subsequently decays to stable ^{55}Mn with a half-life of 2.7 y. ^{55}Fe decays by electron capture with subsequent emission of low-energy x-rays. Most iron in the body is bound to erythrocytes and is hence carried around the body with blood (*28*). It has previously been stated that ^{55}Fe could pose an additional radiation dose (*29*) after in vivo decay of ^{55}Co. This possibility has, however, been disputed, and a radiation dose contribution from ^{55}Fe with realistic injected activities of ^{55}Co is estimated to be around 1% of the ^{55}Co dose if all ^{55}Fe is retained in the body, neglecting biologic excretion. The total radiation dose from ^{55}Fe is hence believed to be negligible (*30*).

Previously, the highest known affinity for SSTR2 was found in vitro for [^{55}Co]Co-DOTATOC. The high affinity was not directly demonstrated in our data, but a nonsignificant increased uptake rate from 0 to 1 h after injection of [^{55}Co]Co-DOTATATE, compared with [^{68}Ga]Ga-DOTATATE, was found, supporting previous findings (*13*) and suggesting that [^{55}Co]Co-DOTATATE has a higher affinity for SSTR than does [^{68}Ga]Ga-DOTATATE.

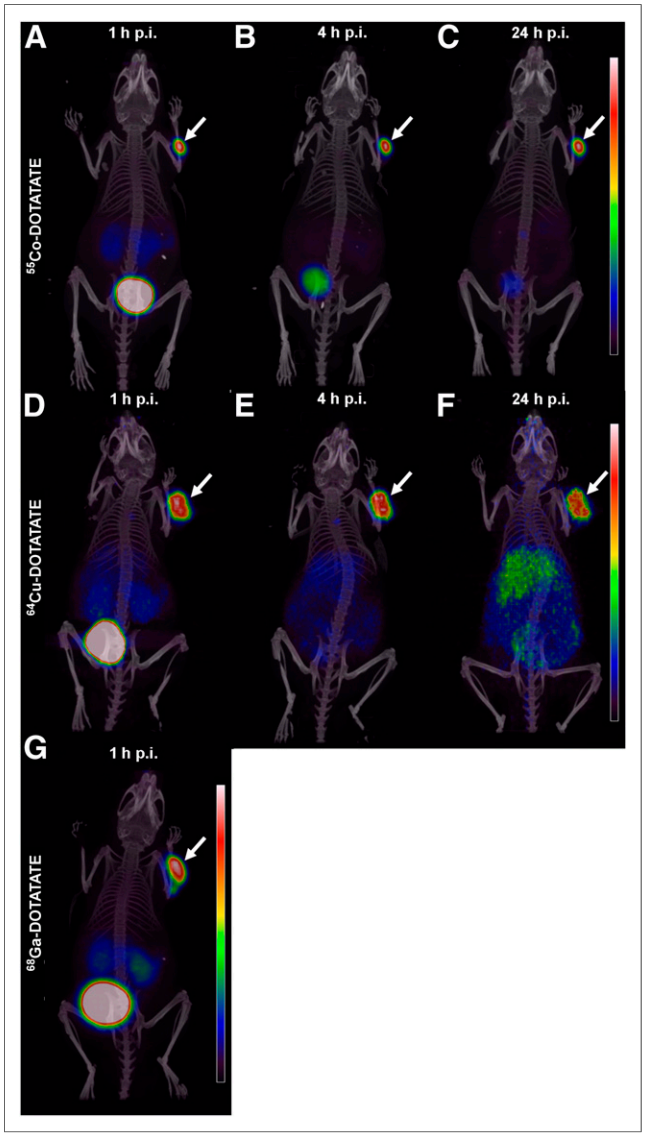

FIGURE 2. Representative maximum-intensity projection from PET/CT scans comparing [^{55}Co]Co-DOTATATE (A–C), [^{64}Cu]Cu-DOTATATE (D–F), and [^{68}Ga]Ga-DOTATATE (G). Arrows indicates tumor in each animal. Decrease in background was observed for [^{55}Co]Co-DOTATATE for late imaging. Higher relative liver uptake with time was observed for [^{64}Cu]Cu-DOTATATE, whereas high bladder uptake was observed for [^{68}Ga]Ga-DOTATATE. All images are scaled to maximum uptake in tumor.

Late-time-point imaging to allow clearance of activity from normal tissues with [^{55}Co]Co-DOTATATE and [^{64}Cu]Cu-DOTATATE at 24 h after injection proved to provide very little gain from imaging at 4 h, based on tumor uptake alone. For [^{64}Cu]Cu-DOTATATE, a nonsignificant decrease in the tumor-to-liver ratio was observed, suggesting a concentration increase of free ^{64}Cu due to [^{64}Cu]Cu-DOTATATE instability, resulting in higher liver uptake with time (Figs. 2D–2F). The ^{64}Cu-DOTA complex is known to undergo transchelation in vivo (*31,32*), leading to activity retention in the liver (*33*), which agrees with our findings (Figs. 2D–2F). In contrast, [^{55}Co]Co-DOTATATE appeared extremely stable in vivo, with statistically significant higher ratios for tumor to liver, tumor to kidney, and tumor to muscle, along with comparable tumor uptake. As such, a decrease in general background was found for [^{55}Co]Co-DOTATATE over time, favoring imaging at 24 h. Conversely, a tumor uptake decrease over time resulted in maximum ratios for tumor to liver and tumor to muscle at 4 h. Only with regard to the tumor-to-kidney ratio was imaging at 24 h beneficial. The very high tumor-to-kidney ratio for imaging at very late time points opens up new possibilities for imaging of SSTR, such as imaging of SSTR-positive renal cell carcinomas, which previously has been difficult because of the high kidney and bladder uptake with normal excretion (*34–36*).

CONCLUSION

The somatostatin analog [^{55}Co]Co-DOTATATE is a promising tracer for PET imaging of SSTR-expressing tumors. The fast clearance of [^{55}Co]Co-DOTATATE from normal tissues resulted in significantly higher tumor-to-background ratios than what was observed for [^{64}Cu]Cu-DOTATATE and [^{68}Ga]Ga-DOTATATE. Importantly, from 4 h after injection, uptake of [^{55}Co]Co-DOTATATE in the tumor was at least 50 times higher than that in the liver, which is a major site of metastasis for NETs. Thus, [^{55}Co]Co-DOTATATE provides excellent image contrast and warrants further development for translation into the clinic.

DISCLOSURE

The bioimaging experiments reported in this paper were performed at DaMBIC, a bioimaging research core facility at the University of Southern Denmark. DaMBIC was established by an equipment grant from the Danish Agency for Science Technology and Innovation and by internal funding from the University of Southern Denmark. No other potential conflict of interest relevant to this article was reported.

KEY POINTS

QUESTION: Can [^{55}Co]Co-DOTATATE improve PET/CT image contrast by delayed imaging compared with [^{64}Cu]Cu-DOTATATE and [^{68}Ga]Ga-DOTATATE in somatostatin-positive tumors?

PERTINENT FINDINGS: [^{55}Co]Co-DOTATATE provides a statistically significant improvement in image contrast in NOD-SCID mice bearing subcutaneous SSTR-expressing AR42J tumors, as exemplified by the tumor-to-liver, tumor-to-kidney, and tumor-to-muscle ratios. Delayed imaging with [^{55}Co]Co-DOTATATE hence offers image contrast superior to either [^{68}Ga]Ga-DOTATATE or [^{64}Cu]Cu-DOTATATE.

IMPLICATIONS FOR PATIENT CARE: The results warrant further translation into clinical practice and hold promise for improved patient diagnostics and future applications for delayed PET/CT imaging.

REFERENCES

1. Rufini V, Calcagni ML, Baum RP. Imaging of neuroendocrine tumors. *Semin Nucl Med.* 2006;36:228–247.
2. Krenning EP, Kwekkeboom DJ, Bakker WH, et al. Somatostatin receptor scintigraphy with [^{111}In-DTPA-D-Phe^{1}]- and [^{123}I-Tyr^{3}]-octreotide: the Rotterdam experience with more than 1000 patients. *Eur J Nucl Med.* 1993;20:716–731.
3. Gabriel M, Decristoforo C, Donnemiller E, et al. An intrapatient comparison of ^{99m}Tc-EDDA/HYNIC-TOC with ^{111}In-DTPA-octreotide for diagnosis of somatostatin receptor-expressing tumors. *J Nucl Med.* 2003;44:708–716.
4. Gabriel M, Decristoforo C, Kendler D, et al. ^{68}Ga-DOTA-Tyr^{3}-octreotide PET in neuroendocrine tumors: comparison with somatostatin receptor scintigraphy and CT. *J Nucl Med.* 2007;48:508–518.
5. Hofmann M, Maecke H, Borner AR, et al. Biokinetics and imaging with the somatostatin receptor PET radioligand ^{68}Ga-DOTATOC: preliminary data. *Eur J Nucl Med.* 2001;28:1751–1757.
6. Kowalski J, Henze M, Schuhmacher J, Macke HR, Hofmann M, Haberkorn U. Evaluation of positron emission tomography imaging using [^{68}Ga]-DOTA-D Phe^{1}-Tyr^{3}-octreotide in comparison to [^{111}In]-DTPAOC SPECT: first results in patients with neuroendocrine tumors. *Mol Imaging Biol.* 2003;5:42–48.
7. Anderson CJ, Pajeau TS, Edwards WB, Sherman ELC, Rogers BE, Welch MJ. In vitro and in vivo evaluation of copper-64-octreotide conjugates. *J Nucl Med.* 1995;36:2315–2325.
8. Förster GJ, Engelbach M, Brockmann J, et al. Preliminary data on biodistribution and dosimetry for therapy planning of somatostatin receptor positive tumours: comparison of ^{86}Y-DOTATOC and ^{111}In-DTPA-octreotide. *Eur J Nucl Med.* 2001;28:1743–1750.
9. Jamar F, Barone R, Mathieu I, et al. ^{86}Y-DOTA^{0})-D-Phe^{1}-Tyr^{3}-octreotide (SMT487): a phase 1 clinical study—pharmacokinetics, biodistribution and renal protective effect of different regimens of amino acid co-infusion. *Eur J Nucl Med Mol Imaging.* 2003;30:510–518.
10. van Essen M, Sundin A, Krenning EP, Kwekkeboom DJ. Neuroendocrine tumours: the role of imaging for diagnosis and therapy. *Nat Rev Endocrinol.* 2014;10:102–114.
11. Antunes P, Ginj M, Zhang H, et al. Are radiogallium-labelled DOTA-conjugated somatostatin analogues superior to those labelled with other radiometals? *Eur J Nucl Med Mol Imaging.* 2007;34:982–993.
12. Reubi JC, Schar JC, Waser B, et al. Affinity profiles for human somatostatin receptor subtypes SST1-SST5 of somatostatin radiotracers selected for scintigraphic and radiotherapeutic use. *Eur J Nucl Med.* 2000;27:273–282.
13. Heppeler A, Andre JP, Buschmann I, et al. Metal-ion-dependent biological properties of a chelator-derived somatostatin analogue for tumour targeting. *Chemistry.* 2008;14:3026–3034.
14. Thisgaard H, Olesen ML, Dam JH. Radiosynthesis of ^{55}Co- and ^{58m}Co-labelled DOTATOC for positron emission tomography imaging and targeted radionuclide therapy. *J Labelled Comp Radiopharm.* 2011;54:758–762.
15. Thisgaard H, Olsen BB, Dam JH, Bollen P, Mollenhauer J, Hoilund-Carlsen PF. Evaluation of cobalt-labeled octreotide analogs for molecular imaging and auger electron-based radionuclide therapy. *J Nucl Med.* 2014;55:1311–1316.
16. Pfeifer A, Knigge U, Mortensen J, et al. Clinical PET of neuroendocrine tumors using ^{64}Cu-DOTATATE: first-in-humans study. *J Nucl Med.* 2012;53:1207–1215.
17. Thisgaard H, Elema DR, Jensen M. Production and dosimetric aspects of the potent Auger emitter ^{58m}Co for targeted radionuclide therapy of small tumors. *Med Phys.* 2011;38:4535–4541.
18. Kirschner A, Ice RD, Beierwaltes WH. Radiation dosimetry of ^{131}I-19-iodocholesterol. *J Nucl Med.* 1973;14:713–717.
19. Basic anatomical and physiological data for use in radiological protection: reference values—a report of age- and gender-related differences in the anatomical and physiological characteristics of reference individuals. ICRP publication 89. *Ann ICRP.* 2002;32:5–265.
20. Siegel JA, Thomas SR, Stubbs JB, et al. MIRD pamphlet no. 16: techniques for quantitative radiopharmaceutical biodistribution data acquisition and analysis for use in human radiation dose estimates. *J Nucl Med.* 1999;40:37S–61S.
21. Stabin MG, Sparks RB, Crowe E. OLINDA/EXM: the second-generation personal computer software for internal dose assessment in nuclear medicine. *J Nucl Med.* 2005;46:1023–1027.

22. Johnbeck CB, Knigge U, Loft A, et al. Head-to-head comparison of ^{64}Cu-DOTATATE and ^{68}Ga-DOTATOC PET/CT: a prospective study of 59 patients with neuroendocrine tumors. *J Nucl Med.* 2017;58:451–457.
23. Pfeifer A, Knigge U, Binderup T, et al. ^{64}Cu-DOTATATE PET for neuroendocrine tumors: a prospective head-to-head comparison with ^{111}In-DTPA-octreotide in 112 patients. *J Nucl Med.* 2015;56:847–854.
24. Junde H. Nuclear data sheets for A=55. *Nucl Data Sheets (NY NY).* 2008;109:787.
25. Singh B. Nuclear data sheets for A=64. *Nucl Data Sheets (NY NY).* 2007;108:197.
26. Braad PEN, Hansen SB, Thisgaard H, Hoilund-Carlsen PF. PET imaging with the non-pure positron emitters: ^{55}Co, ^{86}Y and ^{124}I. *Phys Med Biol.* 2015;60: 3479–3497.
27. Sandström M, Velikyan I, Garske-Roman U, et al. Comparative biodistribution and radiation dosimetry of ^{68}Ga-DOTATOC and ^{68}Ga-DOTATATE in patients with neuroendocrine tumors. *J Nucl Med.* 2013;54:1755–1759.
28. Waldvogel-Abramowski S, Waeber G, Gassner C, et al. Physiology of iron metabolism. *Transfus Med Hemother.* 2014;41:213–221.
29. Pagani M. StoneElander S, Larsson SA. Alternative positron emission tomography with non-conventional positron emitters: effects of their physical properties on image quality and potential clinical applications. *Eur J Nucl Med.* 1997;24: 1301–1327.
30. Paans AMJ, Jansen HML. Dose contribution from iron-55 as a daughter radionuclide of cobalt-55. *Eur J Nucl Med.* 1998;25:445–446.
31. Banerjee SR, Pullambhatla M, Foss CA, et al. ^{64}Cu-labeled inhibitors of prostate-specific membrane antigen for PET imaging of prostate cancer. *J Med Chem.* 2014;57:2657–2669.
32. Garrison JC, Rold TL, Sieckman GL, et al. In vivo evaluation and small-animal PET/CT of a prostate cancer mouse model using ^{64}Cu bombesin analogs: side-by-side comparison of the CB-TE2A and DOTA chelation systems. *J Nucl Med.* 2007;48:1327–1337.
33. Cui C, Hanyu M, Hatori A, et al. Synthesis and evaluation of [^{64}Cu]PSMA-617 targeted for prostate-specific membrane antigen in prostate cancer. *Am J Nucl Med Mol Imaging.* 2017;7:40–52.
34. Kanthan GL, Schembri GP, Samra J, Roach P, Hsiao E. Metastatic renal cell carcinoma in the thyroid gland and pancreas showing uptake on ^{68}Ga DOTATATE PET/CT scan. *Clin Nucl Med.* 2016;41:583–584.
35. Reubi JC, Kvols L. Somatostatin receptors in human renal-cell carcinomas. *Cancer Res.* 1992;52:6074–6078.
36. Höög A, Kjellman M, Mattsson P, Juhlin CC, Shabo I. Somatostatin receptor expression in renal cell carcinoma: a new front in the diagnostics and treatment of renal cell carcinoma. *Clin Genitourin Cancer.* 2018;16:e517–e520.